

**NASA TECHNICAL
MEMORANDUM**

N 71 - 27945
NASA TM X-67838

NASA TM X-67838

**CASE FILE
COPY**

CREEP-FATIGUE ANALYSIS BY STRAIN-RANGE PARTITIONING

by S. S. Manson, G. R. Halford, and M. H. Hirschberg
Lewis Research Center
Cleveland, Ohio

TECHNICAL PAPER proposed for presentation at the First
National Pressure Vessel and Piping Conference sponsored by
the American Society of Mechanical Engineers
San Francisco, May 10 - 12, 1971

CREEP-FATIGUE ANALYSIS BY STRAIN-RANGE PARTITIONING

By S. S. Manson, G. R. Halford, and M. H. Hirschberg

Lewis Research Center

Cleveland, Ohio

SUMMARY

The framework of a new method is outlined for treating creep-fatigue behavior of metals. Cognizance is taken of the fact that inelastic deformation occurs at high temperature as a result of two distinctly different strain-ing mechanisms—plastic flow and creep. Any completely reversed inelastic strain range can then be partitioned into the following components:

- (a) Tensile plastic flow reversed by compressive plastic flow
- (b) Tensile plastic flow reversed by compressive creep, or tensile creep reversed by compressive plastic flow
- (c) Tensile creep reversed by compressive creep

These strain-range components are then related independently to cyclic life by equations which are in essence generalizations of the Manson-Coffin equation. A linear life fraction rule is used to sum the damage resulting from each of these strain-range components. Failure is assumed to occur when the summation of damage fractions equals unity.

Experimental procedures are suggested for obtaining the relationships between cyclic life and each of the partitioned strain ranges. Test results are presented for $2\frac{1}{4}\text{Cr-1Mo}$ steel as well as limited information for 316 stainless steel. The method is used for interpreting effects of frequency of strain cycling and strain hold times in both tension and compression. It also provides insight into the validity of the previously proposed 10 Percent Rule for creep-fatigue analysis.

ABSTRACT

The framework of a new method is outlined for treating creep-fatigue behavior of metals. Inelastic strain-ranges are partitioned into the components (a) completely reversed plasticity, (b) tensile plasticity reversed by compressive creep, or tensile creep reversed by compressive plasticity, and (c) completely reversed creep. Each of these components is shown to be related to cyclic life by a Manson-Coffin type power-law equation. A linear life fraction rule is used to combine the damaging effects of the individual components enabling the prediction of life. Test results are presented for a $2\frac{1}{4}\text{Cr-1Mo}$ steel as well as limited information for a Type 316 stainless steel.

CREEP-FATIGUE ANALYSIS BY STRAIN-RANGE PARTITIONING

By S. S. Manson, G. R. Halford, and M. H. Hirschberg

INTRODUCTION

A number of approaches have in recent years been proposed to treat high-temperature fatigue. Some (refs. 1-9) are extensions of methods developed primarily for treatment of fatigue in the sub-creep range. In these approaches, strain range is the primary correlating variable. Others (refs. 10-18) give prime emphasis to the creep-rupture mechanism involved in high-temperature fatigue. Here the time that the material is at a specified stress, relative to the creep-rupture time at that stress, becomes the principal correlating variable. Each approach has its strong features as well as its limitations, and the search continues for a framework of analysis that includes the strong points of existing methods while overcoming some of the recognized limitations.

Interest in this subject at our laboratory has been intense, and we have participated actively in a continuously evolving method, each modification intended to overcome a recognized limitation of a previous formulation. Our first approach (ref. 4), referred to as the 10 Percent Rule, was based on strain-life relations observed at room temperature, but accounted for the "creep effect" by reducing the life so computed by a factor of 10. This factor was intended to recognize that in the creep range both crack initiation and crack propagation were accelerated by intercrystalline cracking. Remarkably good correlations were obtained in most cases, but it was recognized that this method had no inherent mechanism for including frequency effects. A second method was outlined in Reference 5 which relied on the 10 Percent Rule concept, but also allowed for extreme effects of frequency by incorporating a creep-rupture criterion. At this point, the attempt was still to keep the necessary computations as simple as possible. Better correlations were thereby obtained for continuous cycling tests, but the method did not have the generality required to handle complex wave forms often encountered in practice.

Spera, at our laboratory, in treating thermal stress problems, (refs. 15-17) was concerned with complex temperature and stress variations during the loading cycle. He used a creep damage approach based on the summation of time fractions. This made necessary the determination of the complete stress and temperature history along with the appropriate creep-rupture information to permit a complete analysis. Two important questions arose: (a) which creep-rupture curves should be used, and (b) how should compressive loading be handled? Spera made assumptions regarding both questions, and his analyses have been quite successful for the several problems treated. However, the answers to the above questions still require clarification for a large number of problems encountered in service.

We subsequently evaluated (ref. 18) the applicability of various creep-rupture curves to analyzing high-temperature, strain-cycling fatigue results. Included were the conventional rupture curves for smooth and notched samples and a newly proposed cyclic creep-rupture curve. The latter was derived from tests wherein the creep stresses and strains were completely reversed. For the

two materials studied, the best life predictions were obtained when the cyclic creep-rupture curve was used for analysis. Further study (ref. 19) confirmed the validity of the cyclic creep-rupture curve in correlating cyclic life data for the simple loading cycles used. However, there still remained the problem of handling compression in more complex cycles.

Coffin (ref. 7) modified the equations developed at room temperature for use at high temperature by introducing a frequency modification. Frequency is much more important at high temperature than at room temperature for several reasons. The stress developed is dependent on frequency, and the time dwell at a given stress is, of course, very strongly dependent on frequency; therefore, fatigue properties derived from variable frequency tests inherently reflect the stress magnitude and time-dwell factors. If the proper tests are conducted to characterize the material, good predictions of continuous cycling behavior can be obtained in this manner. However, complex loading histories are still troublesome. For example, the method would predict the same cyclic life for tests incorporating either compressive strain hold periods or tensile strain hold periods. This is contrary to experimental evidence of Berling and Conway (ref. 20).

The above discussion is cited merely to indicate that there still exists a need for a framework of analysis of high-temperature fatigue to overcome some of the unresolved problems. This report is intended to constitute a step in that direction. The basic approach is considerably different from those previously used, although the intent is to build on the good features of those previously proposed methods. The new method is based on the idea of separating cyclic inelastic strains into four possible independent inelastic components. Each type of inelastic strain bears a different relation to life, and once a given imposed strain is partitioned into its components, life is determined according to a linear damage rule. The method is in an early stage of development, and many questions must be answered before its merits can be evaluated.

METHOD

Inelastic strain at high temperature is composed of two distinctly different types of strain—plasticity and creep. Time-independent plastic strain occurs by crystallographic slip within the grains; whereas, time-dependent creep occurs by a combination of diffusion-controlled mechanisms acting within the grains and by sliding along the boundaries between the grains. It is widely accepted that creep mechanisms reduce cyclic life at elevated temperatures. However, there exists in the literature a considerable amount of apparently conflicting evidence regarding the quantitative influence of creep on cyclic life. A careful examination reveals that the life-reducing effects of creep depend, to a large extent, upon where within a cycle the creep is introduced, and whether it is reversed by plastic flow or by creep. Thus, it appears important to distinguish between the various ways in which creep and plastic flow can be combined within a cycle.

Inelastic Strain Components

The method will be described in relation to problems involving only completely reversed inelastic strains; that is, cases which do not involve strain ratcheting in either tension or compression. As will be shown, any one cycle of a completely reversed inelastic strain can be partitioned into the following strain range components:

- (a) $\Delta\epsilon_{pp}$ completely reversed plasticity
- (b) $\begin{cases} \Delta\epsilon_{pc} \\ \Delta\epsilon_{cp} \end{cases}$ tensile plasticity reversed by compressive creep
tensile creep reversed by compressive plasticity or
- (c) $\Delta\epsilon_{cc}$ completely reversed creep

In the above notation, the first letter of the subscript (c for creep and p for plastic strain) refers to the type of strain imposed in the tensile portion of the cycle, and the second letter refers to the type of strain imposed during the compressive portion of the cycle.

In any arbitrary hysteresis loop, such as shown in Figure 1, the tensile inelastic strain (\overline{AD}) can be separated into plastic (\overline{AC}) and creep (\overline{CD}) components. Likewise, the compressive inelastic strain (\overline{DA}) can also be separated into its plastic (\overline{DB}) and creep (\overline{BA}) components. In general, neither the two plastic components (\overline{AC} and \overline{DB}) nor the two creep components (\overline{CD} and \overline{BA}) will be equal. It is only necessary that the entire tensile inelastic strain (\overline{AD}) be equal to the entire compressive inelastic strain (\overline{DA}) since we are dealing with a closed hysteresis loop. The partitioned strain ranges are obtained in the following manner. The completely reversed plastic strain range, $\Delta\epsilon_{pp}$, is the smaller of the two plastic components and in this example is equal to \overline{DB} . The completely reversed creep strain range, $\Delta\epsilon_{cc}$, is equal to the smaller of the two creep components and becomes \overline{CD} . As can be seen graphically, the difference between the two plastic components must be equal to the difference between the two creep components, or $\overline{AC} - \overline{DB} = \overline{BA} - \overline{CD}$. This difference is then equal to $\Delta\epsilon_{pc}$ or $\Delta\epsilon_{cp}$ in accordance with the notation stated above. For this example, it is equal to $\Delta\epsilon_{pc}$ since the tensile plastic strain is greater than the compressive plastic strain. It follows from the above procedure, that the sum of the partitioned strain ranges will necessarily be equal to the total inelastic strain range or the width of the hysteresis loop.

The completely reversed plastic strain, $\Delta\epsilon_{pp}$, and its effect on cyclic life, has been extensively studied. The well-known equation, $N\Delta\epsilon_{pp}^{\infty} = C$, proposed by Manson (ref. 21) and Coffin (ref. 22), provides the form of the life relation under this type of reversed strain. Below the creep range, this is the important damaging inelastic strain. At high temperatures, this may also be the case but only when high frequencies are encountered.

The $\Delta\epsilon_{pc}$ type of strain is often encountered in service as a result of

thermal stress, but has not been clearly identified as such. A high temperature strain-cycling test with compressive hold time also features this type of strain.

The $\Delta\epsilon_{cp}$ strain is analogous to the $\Delta\epsilon_{pc}$ strain, except that the creep is in tension and the plastic strain is in compression. Such a strain component is present in some types of thermal stress problems as well as during strain cycling tests with a hold time in tension.

The effect on cyclic life of completely reversed creep strain, $\Delta\epsilon_{cc}$, has not been fully explored in the past. Material behavior under this type of straining is encountered in cyclic creep-rupture tests (refs. 18-19) as well as in low frequency, high-temperature, reversed-loading fatigue tests.

Strain Range - Life Relations

It is assumed that a unique relation exists between cyclic life and each one of the strain components listed. Although the method does not rely on a specific form for these relations, we shall assume from the limited information at hand that they are of the same form as the Manson-Coffin relation. It is now necessary to consider the types of tests that will reveal these relationships in a simple manner.

The $\Delta\epsilon_{pp}$ Component.- Methods for determining the life relation as a function of reversed plastic strain are now well established at temperatures below the creep range where lives are insensitive to frequency (ref. 23). At high temperature, however, tests conducted by imposing fixed "plastic strain ranges" often produce widely varying lives, depending on frequency of straining. As the frequency is decreased, more time is available for creep to occur, and hence more of the imposed inelastic strain becomes creep rather than plastic flow. Thus, what we may measure and think of as "plastic flow," because it is inelastic, may not be entirely that at all, but may be a mixture of plastic strain and creep strain. The higher the frequency, the higher will be the component of plastic strain; therefore, at high temperature, a real measure of the life relation with a plastic strain component can only be obtained by imposing the frequency at a high enough value to exclude the probability of introducing a large creep component. Frequencies of the order of 0.1 Hz were found to be adequate for the $2\frac{1}{4}\text{Cr}-1\text{Mo}$ steel tested in this investigation. Other materials tested at other temperatures may require higher or lower frequencies.

One way to determine if the frequency is high enough is to run tests over a range of frequencies, and to note the frequency at which life approaches an asymptotic value. The experimentally observed fact that an asymptotic value does indeed tend to be reached lends support to the validity of this strain partitioning concept. It is probably desirable, however, to avoid extremely high (ultrasonic) frequencies because the nature of localized strain distribution may become fundamentally different in this range (ref. 24).

The measured cyclic life of a test run at a sufficiently high frequency will be referred to as N_{pp} . A straight line fit of $\log(\Delta\epsilon_{pp})$ vs. $\log(N_{pp})$

establishes the desired relationship.

A representative hysteresis loop of this kind of cycle is shown in Figure 2(A). In cycling between the strain limits indicated at points A and C, a loop is generated having an inelastic width of the amount \overline{BD} . If this loop is generated below the creep limit or at a frequency high enough to preclude creep at some high temperature then \overline{BD} becomes identically equal to $\Delta\epsilon_{pp}$.

The $\Delta\epsilon_{pc}$ Component.- Several types of tests are possible for determining the relation between $\Delta\epsilon_{pc}$ and life. We shall consider three different ones. The first is run at a constant temperature in the creep range.

Tensile straining is applied at a high rate to insure that plastic strain rather than creep strain occurs during this half of the cycle. The compressive portion of the cycle involves a hold period at a constant stress so that the compressive creep strain can be easily recognized and measured. An example of this kind of a cycle is shown in Figure 3(A). The tensile plastic strain is given by \overline{EB} , the compressive creep strain by \overline{FE} , and a small amount of compressive plastic strain, \overline{BF} , is also indicated. $\Delta\epsilon_{pc}$ for this example becomes equal to \overline{EF} , and $\Delta\epsilon_{pp}$ equals \overline{FB} .

The second type of test also involves a constant temperature in the creep range. Both rapid tensile and compressive straining are imposed, but a hold period at constant peak compressive strain is introduced during which compressive stress relaxation occurs. As the stress relaxes, the corresponding elastic strain is converted to compressive creep strain. In this case, $\Delta\epsilon_{pc}$ equals the amount of stress relaxed divided by the modulus of elasticity. An example of this type of cycle is shown in Figure 3(B). Here, the $\Delta\epsilon_{pc}$ is given by \overline{EF} , and the $\Delta\epsilon_{pp}$ by \overline{FB} .

A third type of test is a modification of the first one described. In this case, the temperature during tensile straining is reduced to a value below the creep range of the material. This then gives added assurance that all the tensile straining is plastic.

A component of completely reversed plastic strain, $\Delta\epsilon_{pp}$, although undesirable, is usually present in the above tests. Ideally, a test to determine the $\Delta\epsilon_{pc}$ -life relation should contain no $\Delta\epsilon_{pp}$, and thus the measured life would be N_{pc} . With a $\Delta\epsilon_{pp}$ component present, the measured life, N , is less than N_{pc} . The life N_{pc} must therefore be computed. This computation cannot be made until the $\Delta\epsilon_{pp}$ - N_{pp} relation has been established. If we assume that the damage associated with the $\Delta\epsilon_{pp}$ term is given by the cycle ratio N/N_{pp} , and likewise the damage associated with the $\Delta\epsilon_{pc}$ term is given by the cycle ratio N/N_{pc} , then assuming a linear life fraction rule we get

$$N/N_{pp} + N/N_{pc} = 1 \quad (1)$$

Having measured $N, \Delta \epsilon_{pp}, \Delta \epsilon_{pc}$, and having established N_{pc} , Equation (1) can be solved for N_{pc} . A straight line fit of $\log(\Delta \epsilon_{pc})^{pp}$ vs. $\log(N_{pc})$ provides the desired relationship.

The $\Delta \epsilon_{cp}$ Component.—The types of tests available for determining the $\Delta \epsilon_{cp}$ —life relationship are identical to those discussed above ($\Delta \epsilon_{pc}$) with a single but very important exception: the conditions under which the tensile and compressive strains are applied must be interchanged. Here again, a component of $\Delta \epsilon_{pp}$ is always present. The damage that is attributed to this type of strain range is given by the cycle ratio N/N_{cp} . The damage associated with the $\Delta \epsilon_{cp}$ term is N/N_{cp} where N_{cp} would be the life associated with a test containing only a $\Delta \epsilon_{cp}$ term. Again, assuming a linear life fraction rule, we obtain

$$N/N_{pp} + N/N_{cp} = 1 \quad (2)$$

Having measured $N, \Delta \epsilon_{pp}, \Delta \epsilon_{cp}$, and having established N_{cp} , Equation (2) can be solved for N_{cp} . A straight line fit of $\log(\Delta \epsilon_{cp})^{pp}$ vs. $\log(N_{cp})$ provides the desired relation. Examples of both types of these cycles are shown in Figure 4(A) and (B). In both of these examples, $\Delta \epsilon_{cp}$ is given by \overline{FB} , and $\Delta \epsilon_{pp}$ by \overline{EF} .

The $\Delta \epsilon_{cc}$ Component.—Two types of tests can be useful in determining the relation between cyclic life and completely reversed creep strain: the cyclic creep-rupture test, and the strain cycling test in which hold periods are introduced at both maximum tensile and compressive strains. Ideally, these tests should be run with all the inelastic strain being creep strain, and the measured life would therefore be N_{cc} . This turns out to be impractical since it would require both tensile and compressive stresses at or below the yield stress. The creep rates would therefore be very low resulting in excessively long test times. Raising the stresses to a more practical level introduces plastic strains. If the plastic strain in tension is exactly equal to the plastic strain in compression, the total inelastic strain in the cycle will be partitioned into $\Delta \epsilon_{pp}$ and $\Delta \epsilon_{cc}$. If, however, the plastic strain in tension is not equal to the plastic strain in compression, then an additional strain component is present being either $\Delta \epsilon_{cp}$ or $\Delta \epsilon_{pc}$. Figure 1 shows an example of such a cycle in which $\Delta \epsilon_{pp}, \Delta \epsilon_{pc}$, and $\Delta \epsilon_{cc}$ are all present. It is because of the unavoidable presence of these strain ranges that the $\Delta \epsilon_{cc}$ —life relation must be the last one to be evaluated. N_{cc} can now be computed from the following equation involving three cycle ratios.

$$N/N_{pp} + N/N_{pc} + N/N_{cc} = 1$$

or

$$N/N_{pp} + N/N_{cp} + N/N_{cc} = 1 \quad (3)$$

whichever is applicable.

Having measured N , $\Delta \epsilon_{pp}$, $\Delta \epsilon_{pc}$ or $\Delta \epsilon_{cp}$, $\Delta \epsilon_{cc}$, and having established N_{pp} , N_{pc} or N_{cp} , Equation 3 can be solved for N_{cc} . The required relationship is then obtained by fitting a straight line to the $\log(\Delta \epsilon_{cc})$ vs. $\log(N_{cc})$ plot. Examples of hysteresis loops resulting from the above mentioned types of cycles are shown in Figures 5(A) and (B). In Figure 5(A), $\Delta \epsilon_{cc}$ is given by the smaller of the two creep strains, or \overline{GB} . $\Delta \epsilon_{pp}$ is the smaller of the two plastic strains, or, \overline{HB} . $\Delta \epsilon_{pc}$ must be the difference between the total inelastic strain, \overline{EB} , and $\Delta \epsilon_{pp} + \Delta \epsilon_{cc}$. In this case, $\Delta \epsilon_{pc} = \overline{EB} - \overline{HB} - \overline{GB}$. The loop shown in Figure 5(B) has been drawn to illustrate a case in which no $\Delta \epsilon_{pc}$ or $\Delta \epsilon_{cp}$ is present. For this example, $\Delta \epsilon_{cc} = \overline{GB}$ and $\Delta \epsilon_{pp} = \overline{EG}$.

Damage Summation

The concept behind strain partitioning as an aid in summing damage components has already, in effect, been applied in the previous section, for example in Equations (1-3). Here the partitioning of an applied strain range into its components was used to determine the relation between cyclic life and one of the strain components, the reversed creep. Having once determined the life relationships for all of the components, the procedure can be reversed. Determine by measurement, calculation, or by estimation, each of the strain components in the repeated inelastic strain cycle of interest. From the individual strain range-life relations, the lives associated with these partitioned strain ranges can be obtained. The damage at failure due to each of the partitioned strain ranges is taken as the cycle ratio: N/N_{pp} , N/N_{pc} , N/N_{cp} , and N/N_{cc} . By substituting these ratios into Equation 3, the predicted number of cycles to failure, N , can be obtained.

EXPERIMENTAL DETAILS

Materials

Two materials were used in this investigation. A major portion of the data were obtained using a Cr-Mo pressure vessel steel. Specimens were cut from an extruded pipe of fully annealed $2\frac{1}{4}$ Cr-1Mo steel (ASTM A335, Grade P22) furnished by the Metal Properties Council. A number of other research laboratories have been supplied with sections of this pipe for other investigations. Details regarding composition and microstructure are documented in Reference 25. Preliminary test results were also obtained using a Type 316 stainless steel. Specimens were machined from hot rolled and annealed bar stock.

Specimens and Heating Techniques

All the specimens used in this investigation were of the thin walled, hourglass, tubular type described in detail and shown in Figure 8 of Reference 23. Two heating methods were used. A major portion of the tests conducted were performed at constant temperature using a silicon carbide heating element inserted inside the tubular specimen as described in Reference 23. Tests run with a step change in temperature during each cycle employed direct resistance heating in conjunction with water cooled specimen grips. This facilitated rapid

changes in temperature. Temperature changes were always performed under zero load. Thermocouples were used for temperature measurement and control in the same manner as described in Reference 23.

Equipment and Test Procedures

A major portion of the equipment and procedures used to generate the data for this investigation are described in detail in Reference 23. Only the new or modified equipment and procedures will be included here. These modifications were necessary only for those tests involving creep under constant load. In these tests, load was servo-controlled until a creep strain limit was reached. When this strain limit was reached, one of two possible procedures was followed. In the case of isothermal tests, the load was reversed. In tests involving step changes in temperature, the load was first brought back to zero, the temperature changed, and the reverse load applied. The procedure described above calls for step changes in load. To prevent load overshoot and to limit the rate of straining to a reasonable level, the oil supplied to the hydraulic actuator was throttled down with a needle valve.

EXPERIMENTAL RESULTS

All of the test data used to generate the individual inelastic strain range versus life relations were limited to those cases in which the damage due to the strain range of interest was greater than 50 percent. These data will be represented by open symbols whose shape resembles the hysteresis loop of the type of test performed. Tests in which none of the inelastic strain components produced more than 50 percent of the damage were used to confirm the method. These data are represented by closed or solid symbols. Again, the shape of the symbol indicates the type of test. Table 1 defines all the symbols used to represent the different inelastic strain ranges consistent with the type of test used to obtain this information.

$2\frac{1}{4}\text{Cr-1Mo Steel}$

Table 2 summarizes the basic cyclic strain-life data obtained on this material.

Figure 2 shows the plastic strain range versus cyclic life relationship for this material at 1100F (865K). These data points were obtained at the test frequencies indicated. Test frequencies for this material and test temperature were sufficiently high so that there was no life dependency on this variable. According to the line shown in this figure, the life relation is

$$\Delta \epsilon_{pp} = 0.74 N_{pp}^{-0.60} \quad (6)$$

Figure 3 shows the $\Delta \epsilon_{pc}$ versus life relationship. Two different types of tests were used to establish this line (see Table 1). The resultant equation representing this relationship is

$$\Delta \epsilon_{pc} = 2.15 N_{pc}^{-0.91} \quad (7)$$

Figure 4 shows the test results used to obtain the relationship between $\Delta \epsilon_{cp}$ and cyclic life. Only isothermal tensile hold time tests were used to determine this relationship. Attempts were made to obtain data for this same type of cycle but with the plastic flow in compression being applied at a lower temperature. These tests exhibited some localized buckling prior to failure and were therefore not included. It appears that some specimen design modifications will be necessary to eliminate this problem. There was no evidence of buckling in the isothermal tests. The equation representing these data is

$$\Delta \epsilon_{cp} = 0.32 N_{cp}^{-.60} \quad (8)$$

Figure 5 shows results of tests run to obtain the relationship between $\Delta \epsilon_{cc}$ and cyclic life. The only type test used to obtain this relationship was the cyclic creep-rupture test. For this material, only a small amount of reversed creep strain, $\Delta \epsilon_{cc}$, could have been obtained from the cyclic relaxation test. This would have resulted in excessively long test times and was therefore not incorporated in this investigation. The relation resulting from the cyclic creep-rupture tests is

$$\Delta \epsilon_{cc} = 0.76 N_{cc}^{-0.72} \quad (9)$$

The life relationships (eqs. 6-9) are summarized in Figure 6.

Type 316 Stainless Steel

Experimental data needed to generate the partitioned strain range-life relations for this material were, for the most part, obtained from the investigation of Reference 19. A limited number of additional tests were conducted in the regions where existing data were insufficient to obtain the required relationships. Tests were conducted at 1300F (980K) although a few tests were conducted with a lower test temperature of 600F (590K) in one-half of the cycle, analogous to several of the tests performed on the $2\frac{1}{4}$ Cr-1Mo steel. The life relations generated for this material are presented in Figure 7.

DISCUSSION

A Qualitative Evaluation of the Strain Partitioning Approach

Figure 6 shows a summary of the straight line relationships derived from Figures 2-5. In drawing these lines, no attempt was made to impose any type of family relationship, considering the early stage of development of this approach. There was not enough experience available to guide in the selection of a pattern. As more information is developed, it is possible that a useful pattern may evolve, similar to the Universal Slopes approach previously derived (refs. 26-27) from sub-creep temperature data.

It is evident from Figure 6 that for the $2\frac{1}{4}\text{Cr-1Mo}$ steel there is a distinct difference in the life relationship for each inelastic strain component. The difference depends on the mechanism in the tensile portion of the cycle as well as on the mechanism of reversal of the strain. For a given strain range for this material, the least damaging effect would appear to result from reversed plasticity that occurs in the slip planes. Strains involving creep are much more damaging. Other materials may, however, reflect different ordering and spacing among the component lines. Figure 7 shows, for example, some preliminary results for the 316 stainless steel. A large difference in life—a factor of about 15—can be seen between the $\Delta\epsilon_{cp}$ and the $\Delta\epsilon_{pp}$ lines. Since this factor is much greater than that observed for the other material (fig. 6), we shall have to await availability of more data before drawing any general conclusions on the relative damage associated with each type of strain component.

The form of the data shown in Figures 6 and 7 provide interesting qualitative explanations of some trends that are now commonly accepted. They explain, for example, why in strain-cycling fatigue at high temperature, lower frequency is accompanied by lower cyclic life: the longer times at each strain level permits more creep, converting reversed plastic strain to reversed creep strain. This concept also suggests there may be a lower bound on cyclic life as frequency is progressively reduced to the point where nearly all the inelastic strain is creep. Since other approaches, based on time ratios or experimental relations of life with cyclic frequency, have not suggested such a lower bound, this subject bears further study.

The lines of figures 6 and 7 also offer an explanation of why tensile hold times during high-temperature strain cycling are more detrimental than rapid strain cycling: tensile creep which occurs during the hold period is later reversed by compressive plastic flow. For the stainless steel, tensile hold periods would be expected to be particularly detrimental whereas compressive hold periods would have very little effect on life (fig. 7). Hold periods in peak compression may be more damaging in other materials and this is suggested by the results shown in Figure 6 for the $2\frac{1}{4}\text{Cr-1Mo}$ steel. Figures 6 and 7 also provide a guide as to what to expect for hold periods in both tension and compression, wherein the line for completely reversed creep strain, $\Delta\epsilon_{cc}$, becomes important.

It has been commonly noted in the literature (see, for example, ref. 20) that strain hold-time effects are greatest when the hysteresis loop is narrow. The proposed approach provides an understanding of these observations. For a narrow hysteresis loop, the additional relaxation creep strain can become a large percentage of the total inelastic strain range of the cycle. The effect of this additional strain can become dominant resulting in a large reduction in life as would be indicated from the results shown in Figures 6 and 7. For a case involving a wide hysteresis loop, the additional relaxation creep strain can be no more than a small percentage of the total inelastic strain range, and will therefore have a minor effect on life.

An interesting application of Figures 6 and 7 relates to the 10 Percent Rule (refs. 4-6) previously studied at our Laboratory. It can be seen from Figure 6 that, for a given strain range, the life can vary about a factor of 10 depending upon the type of strain component featured in the deformation. The highest life can be expected if the strain is all reversed plasticity, and this life estimate can be made on the basis of the Universal Slopes Method. For most materials, it will be accurate within a factor of 2 or 3 (ref. 27). Reducing this estimated life by a factor of 10 (as required by the 10 Percent Rule) will embrace the life, regardless of the type of strain component which really develops, within reasonable accuracy. Thus, it is remarkable how well the 10 Percent Rule works out, considering that it is subject to error both in the initial estimate of the plasticity-life relation based only on static tensile properties, and in its non-commitment as to the type of strain that develops. However, the diverging curves of Figures 6 and 7 suggest that caution should be exercised in applying the 10 Percent Rule at lives above approximately 10^7 cycles to failure.

A Quantitative Evaluation of the Strain Partitioning Approach

A measure of how well the strain partitioning approach and the 10 Percent Rule work out for the data generated in this program can be seen in Figures 8 and 9. In Figure 8, all the data points generated in this study for the $2\frac{1}{4}\text{Cr-1Mo}$ steel are shown on the basis of experimental life vs. predicted life. Two types of data points are shown: those which were used to generate the strain-life relations shown in Figures 2-5, and auxiliary test points not used in these figures. Very good agreement (within a factor of 2) is seen between the predicted and experimental lives. For the open symbols, this, in part, is to be expected because the predictions are based on correlations generated from the very data which enter into the final analysis. But the data points are many, and the types of tests involved are diverse. Thus, the good correlation shown, which is based on only a few empirical constants, is encouraging. The closed symbols, based on tests not used in the determination of the material constants, also show good agreement, which is even more encouraging.

The correlation based on the 10 Percent Rule is shown in Figure 9. In this type of representation, an upper bound line is plotted; determined solely from the tensile properties reported in Reference 25. A lower bound line is plotted, based on the upper bound line, and displaced downward by a factor of 10. An average line, displaced upward by a factor of 2 above the lower bound is drawn. According to the 10 Percent Rule, we expect the data to fall within the upper and lower bounds, being most dense along the average line. It is seen that the 10 Percent Rule is quite good in this case, considering that it required knowledge only of tensile strength, elastic modulus, and reduction of area from a tensile test. Why this is so is now better understood, and under what conditions we can expect greater deviations between predicted and experimental results can now perhaps better be estimated on the basis of the results of the strain partitioning approach.

Metallography

The separation of a total inelastic strain range into its four basic components also opens areas of study regarding the metallurgical differences associated with these components. Figure 10 shows micrographs of the failure section of 316 stainless steel specimens for two types of strain component, $\Delta \epsilon_{cp}$ and $\Delta \epsilon_{pc}$ at two strain levels. Figures 10(A) and (B) refer to the high strain. Note that the failure section associated with the tensile creep reversed by plastic flow ($\Delta \epsilon_{cp}$) is completely intergranular, while for approximately the same strain range the failure is completely transgranular if the tension is plastic and the compression is creep ($\Delta \epsilon_{pc}$). The lives are correspondingly different: tensile creep results in only 15 cycles of life for this strain range; compressive creep results in 264 cycles. The results for a lower strain range are shown in Figures 10(C) and (D). Again, tensile creep reversed by compressive plastic flow results in intercrystalline failure, while compressive creep reversed by tensile plastic flow shows no intercrystalline cracking. For the tensile creep test, the life was 632 cycles; for the test involving tensile plastic flow and compressive creep, the specimen had not yet failed after 3070 cycles when the test was discontinued. Transcrystalline surface cracks had started, but continuity among adjacent interior crystals remained intact.

Photomicrographs of tested specimens of the $2\frac{1}{4}\text{Cr}-1\text{Mo}$ steel are shown in Figure 11. Detailed examination reveals trends in cracking behavior that are similar to those found for the Type 316 stainless steel. However, the high degree of oxidation of this material at 1100F (865K) hinders the clear identification of the mode of surface cracking. The micrographs of the specimens shown in Figures 11(A) and (C) indicate only transgranular cracking. These specimens were subjected to tensile plastic flow reversed by compressive creep. Figures 11(B) and (D), on the other hand, show mixed intergranular and transgranular cracking. Here, tensile creep was reversed by compressive plastic flow. In contrast to the behavior of the Type 316 stainless steel, no subsurface intergranular cracking was visible, thus suggesting that tensile creep reversed by compressive plastic flow is not as damaging for this material as for the stainless steel. This difference in behavior is also reflected by the difference between the $\Delta \epsilon_{cp}-N_{cp}$ relationships for these two materials. It should be noted that the lives listed in Figures 11(B) and (D) are approximate since these specimens experienced some localized buckling prior to failure.

This metallographic study shows that the nature of the imposed inelastic strain--how tensile and compressive creep combine with plastic flow to absorb an imposed strain--governs the mechanisms of microstructural deterioration and therefore the life. Such metallurgical studies are valuable and should be extended.

Potential of the Strain Partitioning Method

While the method does not explicitly require a detailed stress analysis, as do for example those methods which are based on the time-fraction procedures, it contains an implicit requirement that the strains be partitioned according to type. Accurate partitioning may become complicated, and may, in fact, still require a complete stress analysis, as well as supplementary material test results. Thus, the merit of the strain partitioning method lies not so much in that it will by-pass the requirement of a complete stress analysis, but in that it will provide a better framework for qualitative reasoning regarding how

loadings will affect life. It resolves the problem of how to treat compressive loading. Lower bounds on life can be estimated, based on the most damaging component of strain, and on an estimate of the fraction of the inelastic strain range that the most damaging component constitutes. How changes in operating conditions will affect the partitioned strain components can also be subjected to qualitative study. Finally, there is a good possibility that when more experience becomes available, the strain-partitioned life relations themselves can be estimated from simpler tests (such as tensile and creep ductilities), thereby greatly increasing the effectiveness of the method as a qualitative tool.

The strain partitioning approach may reduce considerably the complications associated with complex temperature variation and reduce to a secondary role the problem of accurate determination of stress and temperature history. When a time-fraction summation method is used, the stresses and concurrent temperatures must be accurately known, since creep-rupture life is very sensitive to stress and temperature. On the other hand, the strain range partitioning approach recognizes that cyclic life is governed by the capacity of a material to absorb inelastic strain. We have indicated that there are four different ways in which cyclic inelastic strain can be absorbed. Since tensile and creep ductilities are often relatively insensitive to temperature and time to failure, we would anticipate that the curves of Figures 6 and 7 should be no more sensitive to temperature than are these ductilities. For example, the curves of Figure 6 might be applicable over a temperature range of 800F (700K) to 1200F (920K) within a factor of two in life. This result was arrived at from a consideration of the variations in tensile and creep ductilities with temperature reported in Reference 25. This approach might, therefore, be one in which material data is generated at one temperature but is applicable over a range of temperatures.

As presented in this report, the data were limited to relatively-short time exposures (less than 200 hours), thus omitting consideration of metallurgical interactions that could occur as a result of much longer time exposure to stress and temperature. If such exposure is involved in service application, it would be desirable to extend the basic tests into the proper time range. It might also be noted (fig. 6) that at low strain levels, normally associated with the longer cyclic lives, deviations between life governed by completely reversed plastic strain, and life governed by tensile creep reversed by plastic flow, can increase to factors much larger than 10. Differences in life by factors of 100 or 1000 can develop depending on whether an imposed strain is absorbed completely as plastic or creep strain. Thus, the curves need to be experimentally verified in this important low strain region where large reductions in lives can be experienced.

CONCLUDING REMARKS

The recent trend in creep-fatigue analyses has been to consider two independent processes — a "creep effect," dependent mainly on stress-time factors, and a "pure fatigue effect" due to imposed cyclic strain. There has also been a tendency to combine the two effects by a nonlinear cumulative damage law, adding considerably to the complexity of the treatment and to the amount of basic data required for an analysis. The strain-partitioning approach described in this report is an attempt to reduce the entire analysis to a consideration of only strains, although to do so requires the inelastic strain range to be partitioned into several components previously not considered separately. Initial experience is promising—for example, in explaining frequency effects, strain hold-time effects and a possible basis for the 10 Percent Rule. This experience is limited, however, and only further study can reveal the full scope of the opportunities afforded by the approach, or of its limitations.

REFERENCES

1. Coffin, L. F., Jr., "Cyclic Strain and Fatigue Study of a 0.1 pct C-2.0 pct Mo Steel at Elevated Temperatures," Transactions of the AIME, Vol. 230, No. 7, Dec. 1964, pp. 1690-1699.
2. Coffin, L. F., Jr., "An Investigation of the Cyclic Strain and Fatigue Behaviour of a Low-Carbon Manganese Steel at Elevated Temperature," Proceedings of the International Conference on Thermal and High-Strain Fatigue, The Metals and Metallurgy Trust, London, 1967, pp. 171-197.
3. Manson, S. S. and Spera, D. A., "Discussion to The Low-Cycle Fatigue Characteristics of a Nickel-Base Superalloy at Room Temperature by C. H. Wells and C. P. Sullivan," ASM Transactions Quarterly, Vol. 58, No. 4, Dec. 1965, pp. 749-751.
4. Manson, S. S., "Interfaces Between Fatigue, Creep, and Fracture," International Journal of Fracture Mechanics, Vol. 2, No. 1, Mar. 1966, pp. 327-363.
5. Manson, S. S. and Halford, G. R., "A Method of Estimating High-Temperature Low-Cycle Fatigue Behavior of Materials," Proceedings of the International Conference on Thermal and High-Strain Fatigue, The Metals and Metallurgy Trust, London, 1967, pp. 154-170.
6. Halford, G. R. and Manson, S. S., "Application of a Method of Estimating High-Temperature Low-Cycle Fatigue Behavior of Materials," Transactions of the ASM, Vol. 61, No. 1, Mar. 1968, pp. 94-102.
7. Coffin, L. F., Jr., "The Effect of Frequency on High-Temperature Low-Cycle Fatigue," Proceedings of the Air Force Conference on Fatigue and Fracture of Aircraft Structures and Materials. AFFDL TR 70-144, 1970, Air Force Flight Dynamics Lab., Wright-Patterson AFB, Ohio, pp. 301-311.
8. Conway, J. B. and Berling, J. T., "A New Correlation of Low-Cycle Fatigue Data Involving Hold Periods," Metallurgical Transactions, Vol. 1, No. 1, Jan. 1970, pp. 324-325.
9. Berling, J. T. and Conway, J. B., "A New Approach to the Prediction of Low-Cycle Fatigue Data," Metallurgical Transactions, Vol. 1, No. 4, Apr. 1970, pp. 805-809.
10. Taira, S., "Lifetime of Structures Subjected to Varying Load and Temperature," Creep in Structures, N. J. Hoff, ed., Academic Press, New York, 1962, pp. 96-124.
11. Edmunds, H. G. and White, D. J., "Observations of the Effect of Creep Relaxation on High-Strain Fatigue," Journal of Mechanical Engineering Science, Vol. 8, No. 3, Sept. 1966, pp. 310-321.

12. Tilly, G. P., "Influence of Static and Cyclic Loads on the Deformation Behaviour of an Alloy Steel at 600C," Proceedings of the International Conference on Thermal and High-Strain Fatigue, The Metals and Metallurgy Trust, London, 1967, pp. 198-210.
13. Timo, D. P., "Designing Turbine Components for Low-Cycle Fatigue," Presented at International Conference on Thermal Stresses and Thermal Fatigue, Berkeley, England, Sept. 1969.
14. Esztergar, E. P., "Interim Design Basis for Creep and Fatigue Conditions," GA-P-1230-1, July 1969, Gulf General Atomic, Inc., San Diego, Calif.
15. Spera, D. A., "Calculation of Thermal-Fatigue Life Based on Accumulated Creep Damage," TN D-5489, 1969, NASA, Cleveland, Ohio.
16. Spera, D. A., "The Calculation of Elevated-Temperature Cyclic Life Considering Low-Cycle Fatigue and Creep," TN D-5317, 1969, NASA, Cleveland, Ohio.
17. Spera, D. A., Howes, M. A. H., and Bizcn, P. T., "Thermal-Fatigue Resistance of 15 Alloys Determined by the Fluidized-Bed Technique," TM X-52975, 1971, NASA, Cleveland, Ohio.
18. Manson, S. S., Halford, G. R., and Spera, D. A., "The Role of Creep in High-Temperature Low-Cycle Fatigue," A. E. Johnson Memorial Volume, A. I. Smith, ed., Elsevier, Amsterdam, 1971, pp. 229-249.
19. Halford, G. R., "Cyclic Creep-Rupture Behavior of Three High-Temperature Alloys," TN D-6309, 1971, NASA, Cleveland, Ohio.
20. Berling, J. T. and Conway, J. B., "Effect of Hold Time on the Low-Cycle Fatigue Resistance of 304 Stainless Steel at 1200F," First International Conference on Pressure Vessel Technology, Delft, 1969.
21. Manson, S. S., "Behavior of Materials Under Conditions of Thermal Stress," Heat Transfer Symposium, Univ. of Michigan, June 27-28, 1952, Univ. of Michigan Press; also TN 2933, NACA, Cleveland, Ohio.
22. Coffin, L. F., Jr., "A Study of the Effects of Cyclic Thermal Stresses on a Ductile Metal," Transactions of the ASME, Vol. 76, No. 6, Aug. 1954, pp. 931-950.
23. Hirschberg, M. H., "A Low-Cycle Fatigue Testing Facility," Manual on Low-Cycle Fatigue Testing. Spec. Tech. Publ. No. 465, ASTM, Philadelphia 1969, pp. 67-86.
24. Mason, W. P. and Wood, W. A., "Note on Fatigue Mechanisms in fcc Metals at Ultrasonic Frequencies," Tech. Rep. No. 59, Mar. 1968, Dept. of Civil Eng. and Eng. Mech., Columbia Univ., New York City, N. Y., 1968.

25. Jaske, C. E. and Mindlin, H., "Elevated-Temperature Low-Cycle Fatigue Behavior of $2\frac{1}{4}\text{Cr-1Mo}$ and $1\text{Cr-1Mo-}\frac{1}{4}\text{V}$ Steels," presented at the Second Annual Pressure Vessel and Piping Conference, Denver, Colo., 1970.
26. Manson, S. S. and Hirschberg, M. H., "Fatigue Behavior in Strain Cycling in the Low and Intermediate Cycle Range," Fatigue—An Interdisciplinary Approach, J. J. Burke, N. L. Reed, and V. Weiss, eds., Syracuse Univ. Press, Syracuse, N. Y., 1964, pp. 133-173.
27. Manson, S. S., "Fatigue: A Complex Subject—Some Simple Approximations," Experimental Mechanics, Vol. 5, No. 7, July 1965, pp. 193-226.

TABLE 1. - DEFINITION OF DATA SYMBOLS AND NOTATION USED FOR PARTITIONED STRAIN RANGES.


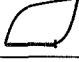
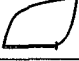




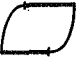

NOTATION	SYMBOL	HYSTERESIS LOOP	DESCRIPTION	
$\Delta\epsilon_{pp}$	○		TENSION PLASTIC COMPRESSION PLASTIC	ISOTHERMAL
$\Delta\epsilon_{pc}$	◻		TENSION PLASTIC COMPRESSION CREEP	ISOTHERMAL
	△		TENSION PLASTIC COMPRESSION CREEP	PLASTICITY AT LOW TEMPERATURE
	◻		TENSION PLASTIC COMPRESSION CREEP (RELAXATION)	ISOTHERMAL
$\Delta\epsilon_{cp}$	◻		TENSION CREEP COMPRESSION PLASTIC	ISOTHERMAL
	▽		TENSION CREEP COMPRESSION PLASTIC	PLASTICITY AT LOW TEMPERATURE
	◻		TENSION CREEP (RELAXATION) COMPRESSION PLASTIC	ISOTHERMAL
$\Delta\epsilon_{cc}$	◻		TENSION CREEP COMPRESSION CREEP	ISOTHERMAL
	◻		TENSION CREEP (RELAXATION) COMPRESSION CREEP (RELAXATION)	ISOTHERMAL

TABLE 2

Experimental Results for $2\frac{1}{4}$ Cr-1Mo Steel

Spec. No.	Symbol	Temp.* Ten/Comp	$\Delta\epsilon_{pp}$	$\Delta\epsilon_{pc}$	$\Delta\epsilon_{cp}$	$\Delta\epsilon_{cc}$	Total Inelastic Strain Range	Observed Cyclic Life
64	○	1/1	.02970	—	—	—	.02970	186
62		"	.03358	—	—	—	.03358	192
49		"	.00774	—	—	—	.00774	1285
31		"	.00204	—	—	—	.00204	13360
35		"	.00226	—	—	—	.00226	25360
53		2/2	.01200	—	—	—	.01200	941
47		"	.00127	—	—	—	.00127	55210
41		3/3	.01990	—	—	—	.01990	267
33	◻	1/1	.01870	.02130	—	—	.04000	158
34		"	.00551	.00169	—	—	.00720	1153
48		"	.00337	.00183	—	—	.00520	2038
16	△	4/1	.01350	.03550	—	—	.04900	88
57		"	.00178	.00645	—	—	.00823	729
46		"	.00256	.00267	—	—	.00523	1473
39	◻	1/1	.00495	—	.00845	—	.00980	449
2		"	.00352	—	.00425	—	.00777	1337
29		"	.00151	—	.00182	—	.00333	5734
26	▽	3/4	.01330	—	.01470	—	.02800	88
23		"	.00443	—	.00090	—	.00533	2455
19	◻	1/1	.00940	—	.00070	—	.01010	796
60		"	.00426	—	.00048	—	.00474	2215
28	◻	1/1	.00810	.00050	—	—	.00860	906
55	◻	1/1	.00250	—	.01180	.02270	.03700	55
45		"	.01621	—	.00180	.03380	.05181	66
61		"	.00848	.00330	—	.02030	.03208	124
3		"	.01880	.00200	—	.02550	.04630	136
18		"	.00190	.00150	—	.01380	.01720	140
56		"	.01266	.00480	—	.01830	.03576	149
52		"	.01630	.00490	—	.00690	.02810	244
63		"	.00325	.00282	—	.00690	.01297	628
6		"	.00362	.00081	—	.00342	.00785	828
51		"	.00320	.00049	—	.00129	.00498	2915
43		3/3	.00889	—	.00213	.00520	.01622	398

*1=1100F (856K) 2=1050F (840K) 3=950F (785K) 4=600F (590K)

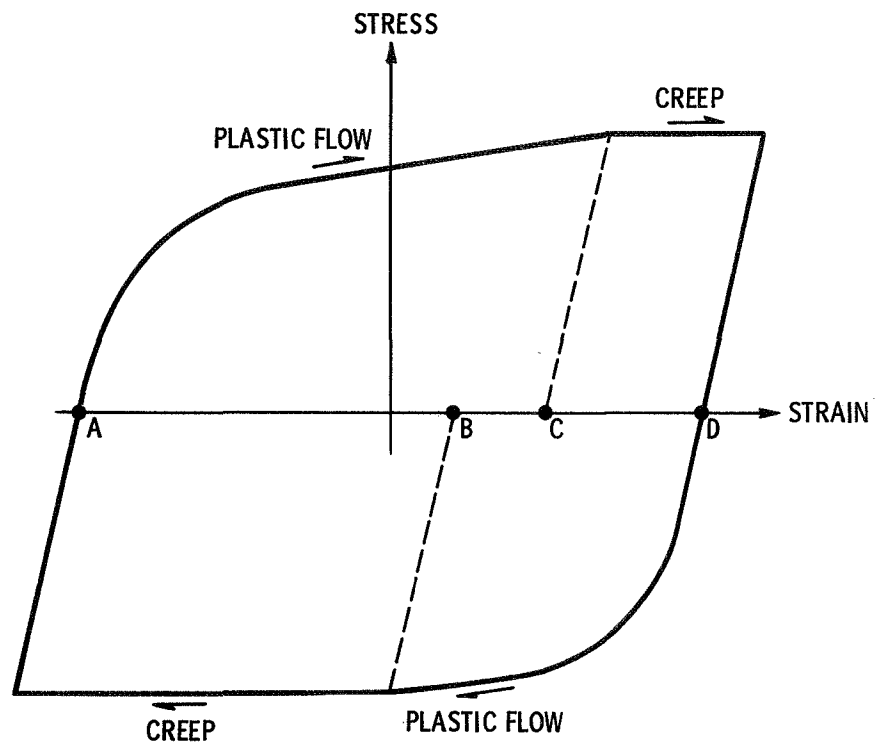


Figure 1. - Hysteresis loop.

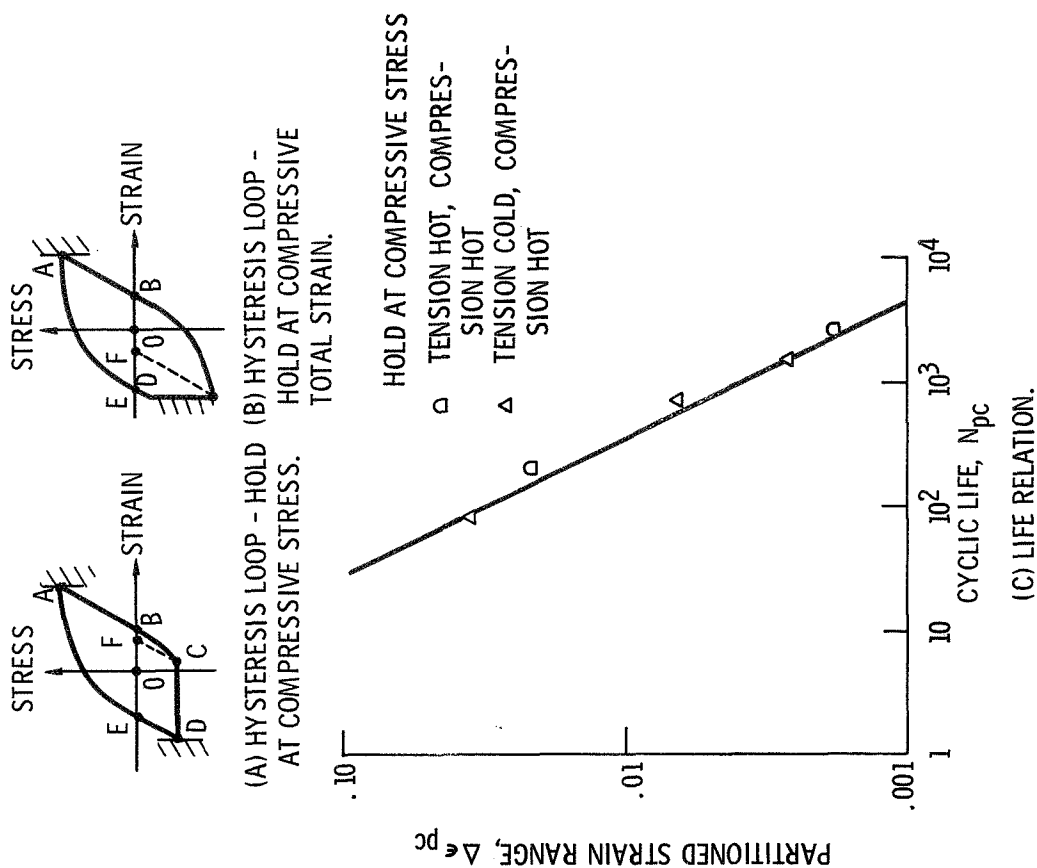


Figure 3. - Life relation for tensile plastic strain reversed by compressive creep strain. $2\frac{1}{4}$ Cr - 1 Mo steel, 1100 F (865 K) and 600 F (590 K).

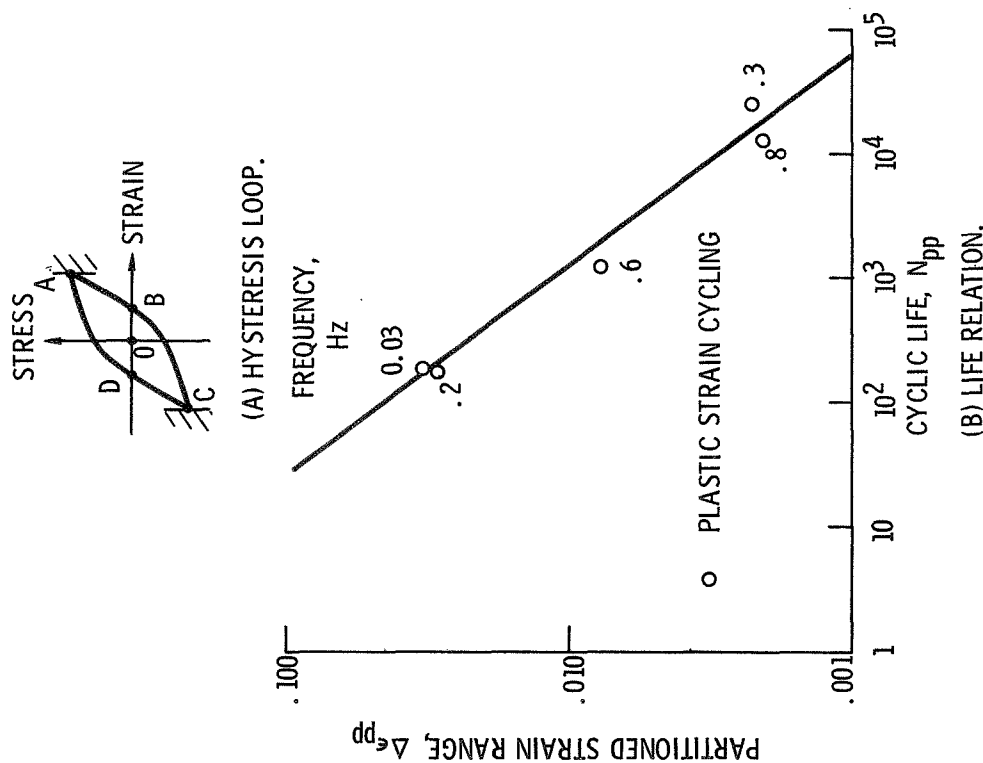
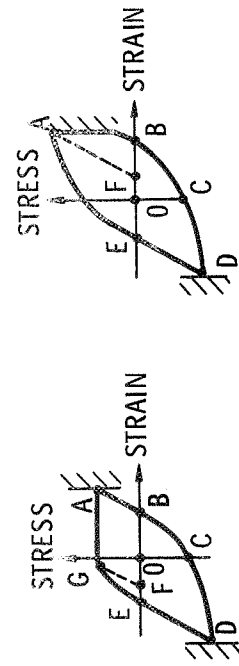


Figure 2. - Life relation for completely reversed plastic strain. $2\frac{1}{4}$ Cr - 1 Mo steel, 1100 F (865 K).



(A) HYSTERESIS LOOP - HOLD AT TENSILE STRESS.
 (B) HYSTERESIS LOOP - HOLD AT TENSILE TOTAL STRAIN.

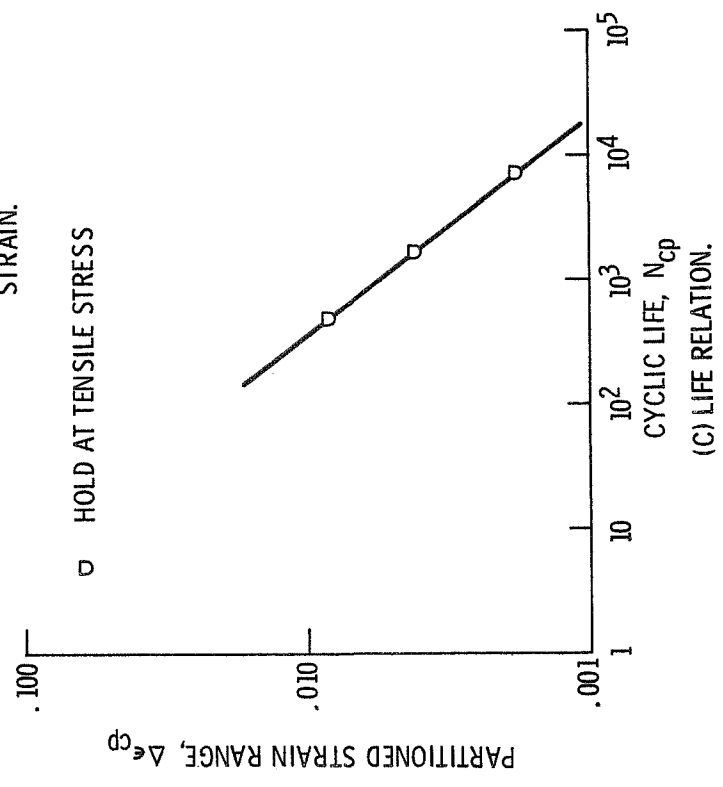
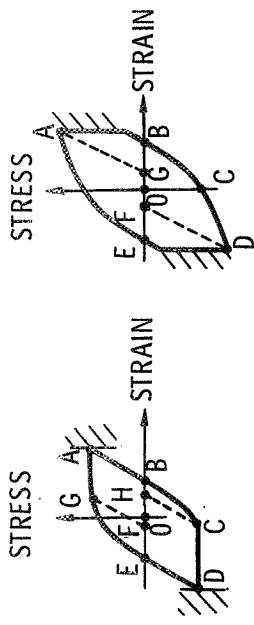


Figure 4. - Life relation for tensile creep strain reversed by compressive plastic strain. $2\frac{1}{4}$ Cr - 1 Mo steel, 1100 F (865 K).



(A) HYSTERESIS LOOP - HOLD AT TENSILE AND COMPRESSIVE STRESSES. GIVE TOTAL STRAINS.
 (B) HYSTERESIS LOOP - HOLD AT TENSILE AND COMPRESSIVE STRESSES. GIVE TOTAL STRAINS.

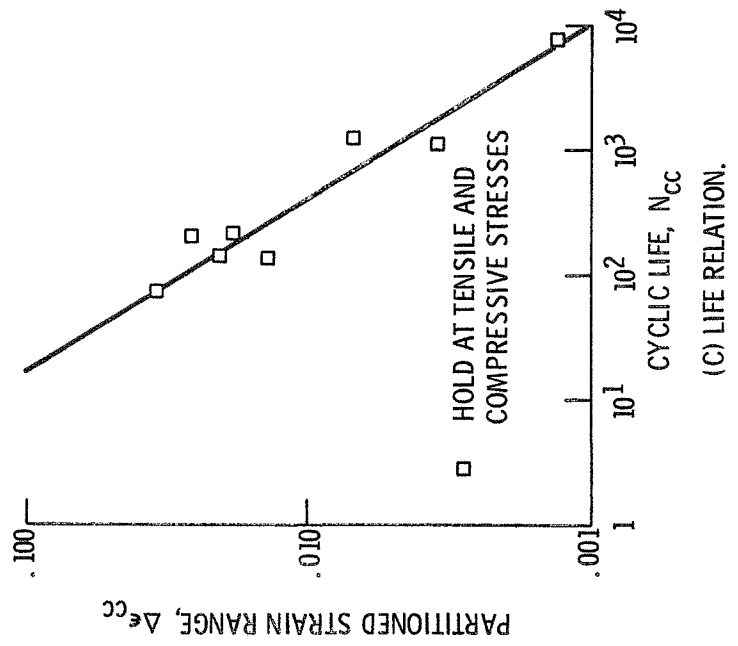


Figure 5. - Life relation for completely reversed creep strain. $2\frac{1}{4}$ Cr - 1 Mo steel, 1100 F (865 K).

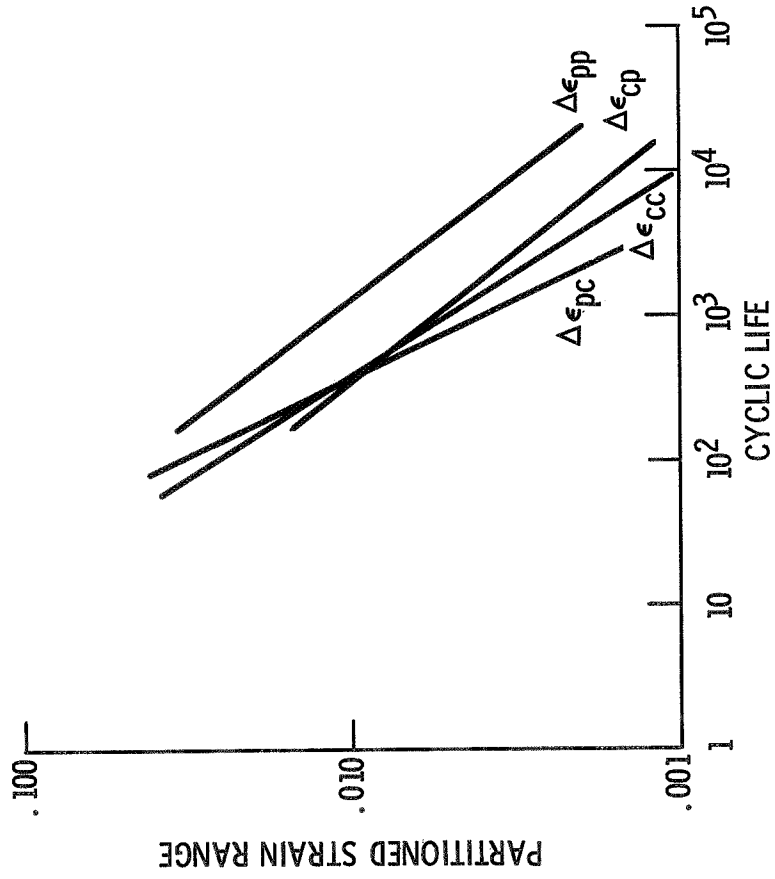


Figure 6. - Summary of partitioned strain-life relations. 2 $\frac{1}{4}$ Cr - 1 Mo steel, 1100 F (865 K).

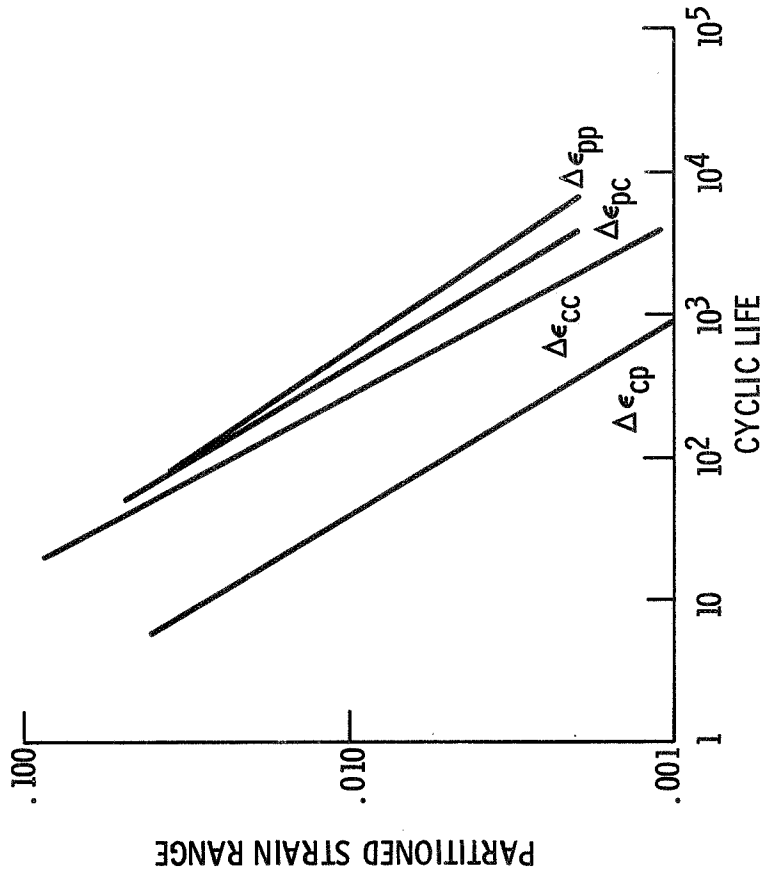


Figure 7. - Summary of partitioned strain-life relations. Type 316 stainless steel, 1300 F (980 K).

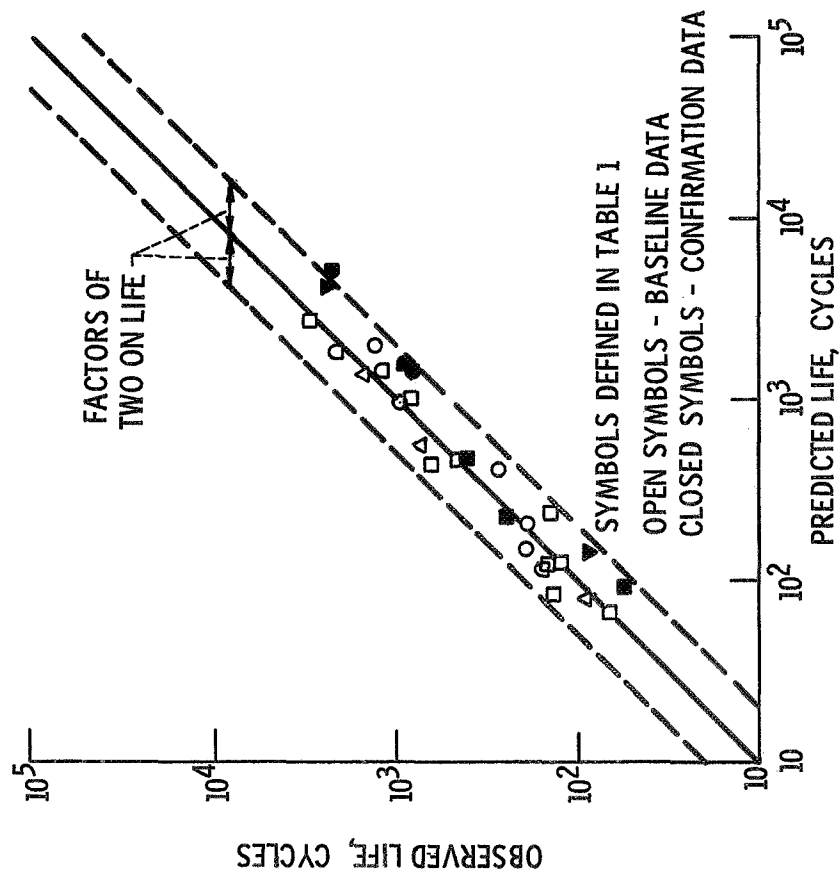


Figure 8. - Summary of life predictability by strain range partitioning. $2\frac{1}{4}$ Cr - 1 Mo steel.

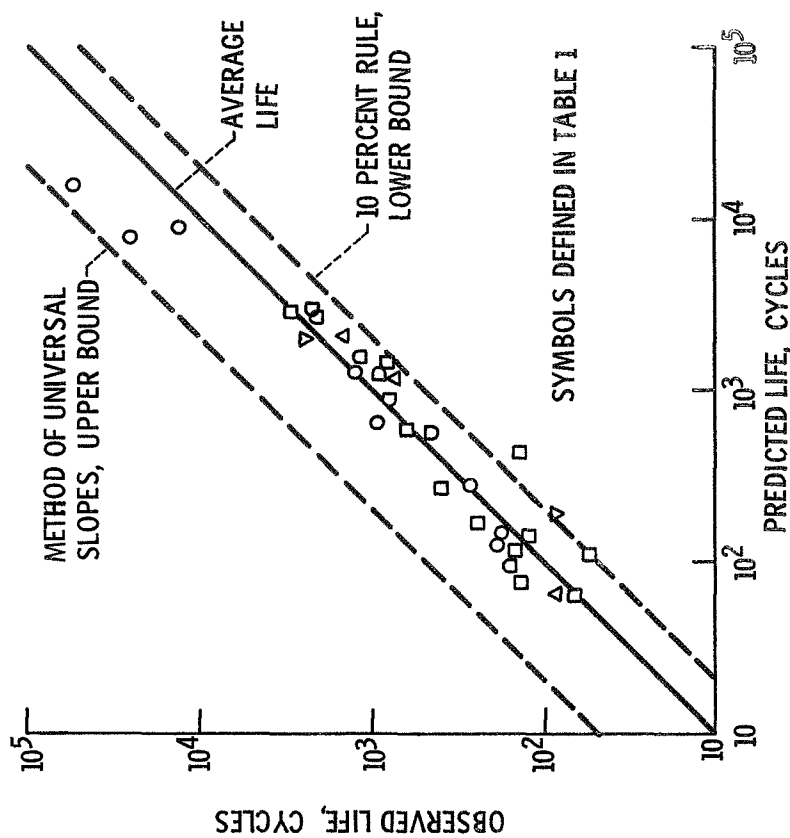
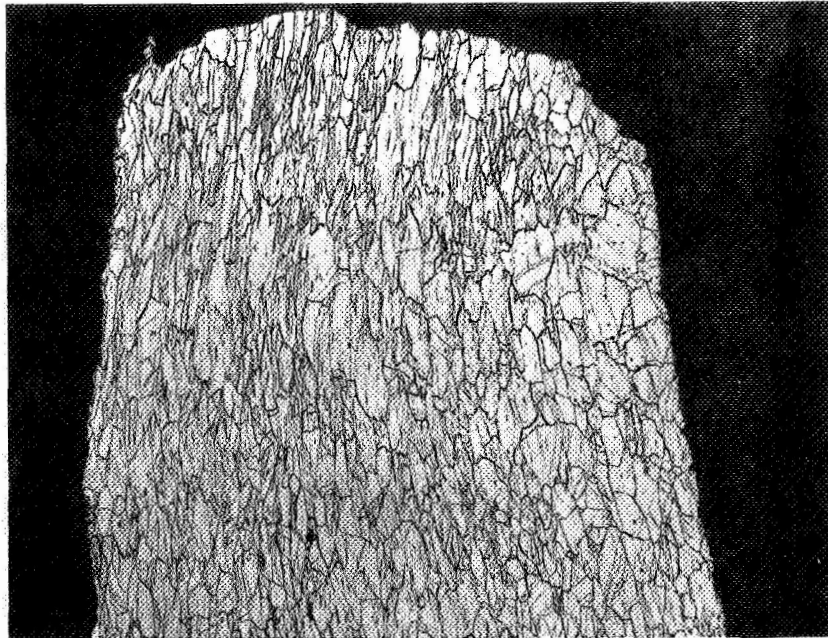
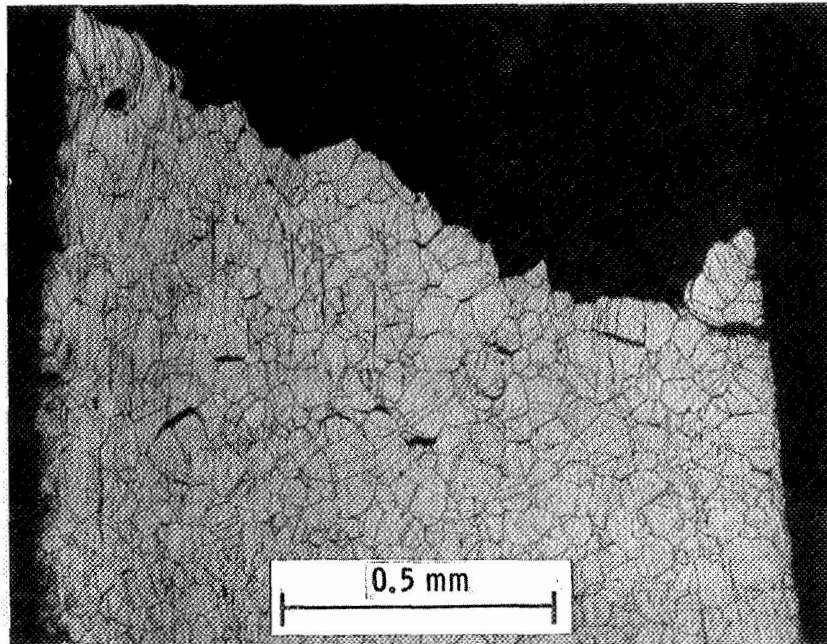


Figure 9. - Summary of life predictability by 10 percent rule. $2\frac{1}{4}$ Cr - 1 Mo steel.

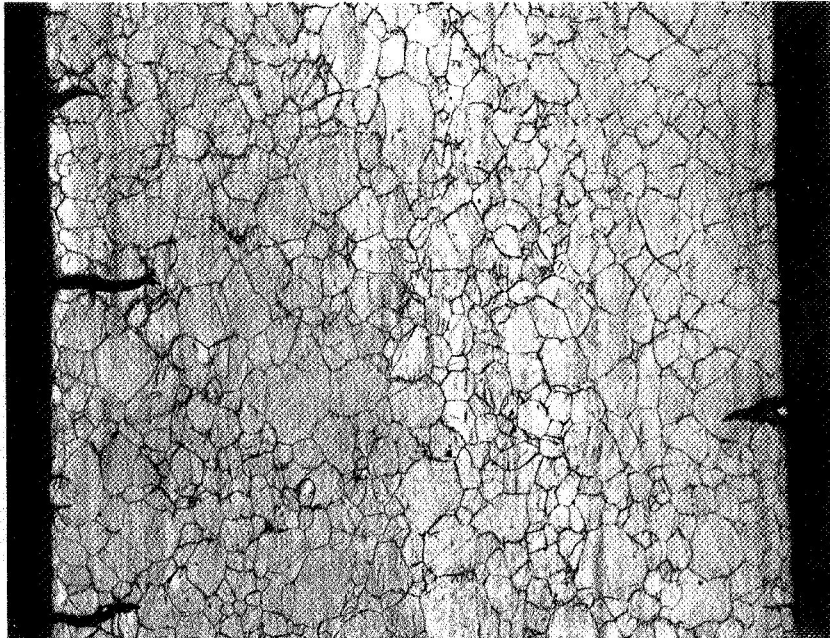


(A) TENSILE PLASTIC FLOW, COMPRESSIVE CREEP.
 $\Delta\epsilon_{pc} = 0.0162$, $N = 264$.

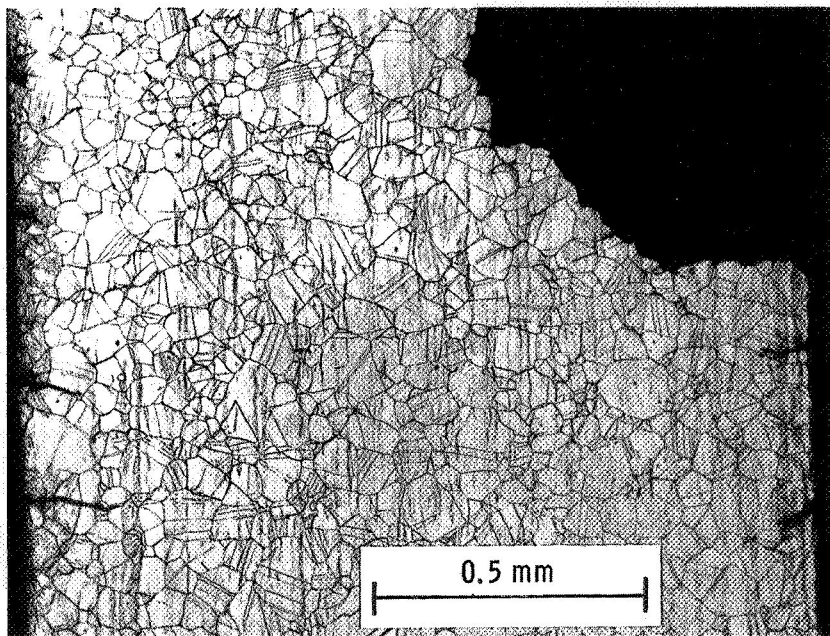


(B) TENSILE CREEP, COMPRESSIVE PLASTIC FLOW.
 $\Delta\epsilon_{cp} = 0.0147$, $N = 15$.

Figure 10. - Photomicrographs of fractured specimens of 316 stainless steel tested in creep-fatigue. Creep at 1300 F (980 K), plastic flow at 600 F (590 K). Outside surface at left, inside surface at right, loading direction vertical.

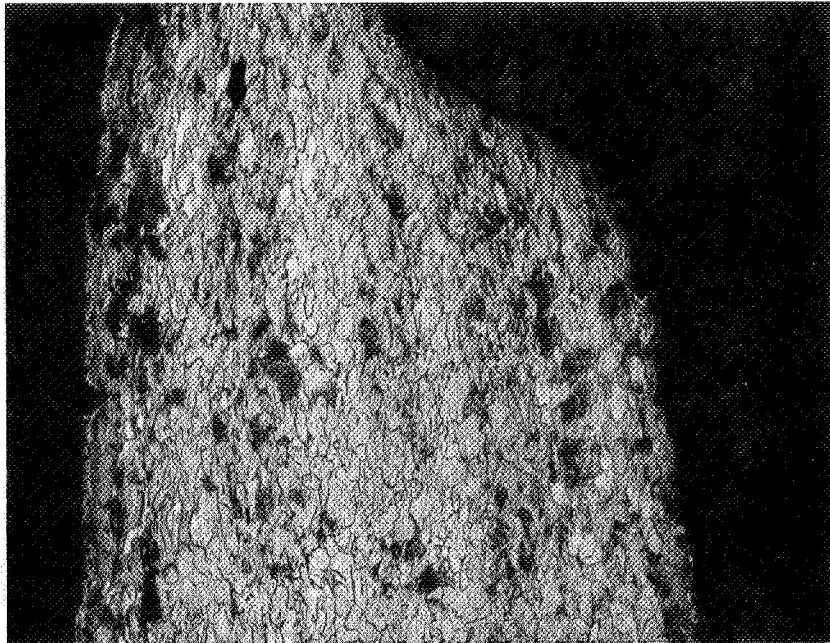


(C) TENSILE PLASTIC FLOW, COMPRESSIVE CREEP.
 $\Delta\epsilon_{pc} = 0.00267$, $N > 3070$.

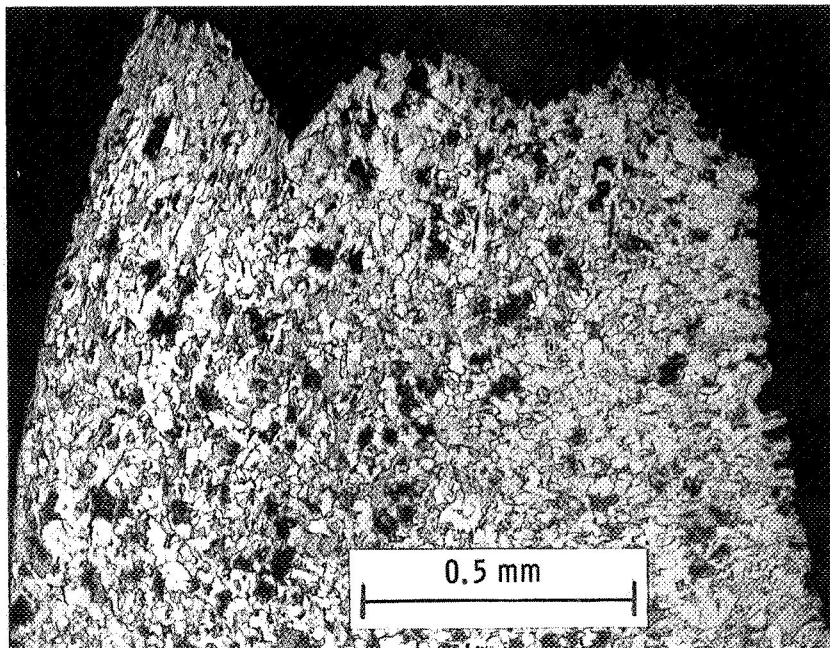


(D) TENSILE CREEP, COMPRESSIVE PLASTIC FLOW.
 $\Delta\epsilon_{cp} = 0.00122$, $N = 632$.

Figure 10. - Concluded.



(A) TENSILE PLASTIC FLOW, COMPRESSIVE CREEP.
 $\Delta\epsilon_{pc} = 0.0355$, $N = 88$.

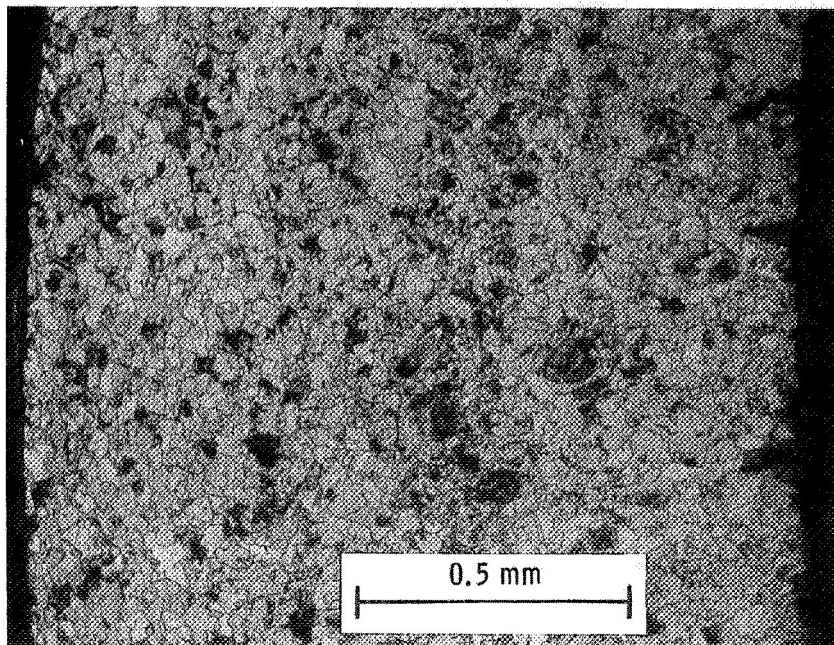


(B) TENSILE CREEP, COMPRESSIVE PLASTIC FLOW.
 $\Delta\epsilon_{cp} = 0.0087$, $N \approx 75$.

Figure 11. - Photomicrographs of fractured specimens of 2 1/4 Cr - 1 Mo steel tested in creep-fatigue. Creep at 1100 F (865 K), plastic flow at 600 F (590 K). Outside surface at left, inside surface at right, loading direction vertical.



(C) TENSILE PLASTIC FLOW, COMPRESSIVE CREEP.
 $\Delta\epsilon_{pc} = 0.00645$, $N = 729$.



(D) TENSILE CREEP, COMPRESSIVE PLASTIC FLOW.
 $\Delta\epsilon_{cp} = 0.00277$, $N \approx 532$.

Figure 11. - Concluded.